Journal of Theoretical and Applied Information Technology
15th April 2022. Vol.100. No 7

ISSN: 1992-8645 www.jatit.org E-ISSN: 1817-3195

COMPARISON OF VARIOUS CONDUCTION MODES FOR THREE-PHASE INVERTER

KRISMADINATA KRISMADINATA[12], IRMA HUSNAINI[12], ASNIL ASNIL[12], REMON LAPISA[2], ROSLI OMAR[3]

[1]Departement of Electrical Engineering, Faculty of Engineering, Universitas Negeri Padang, Indonesia

[2]Centre for Energy and Power Electronics Research (CEPER), Universitas Negeri Padang, Indonesia

[3]Universiti Teknikal Malaysia Melaka, Faculty of Electrical Engineering, Melaka, Malaysia

E-mail: krisma@ft.unp.ac.id, irma_hnni@ft.unp.ac.id, asnil@ft.unp.ac.id, remonlapisa@ft.unp.ac.id, rosliomar@utem.edu.my

ABSTRACT

The root mean square (RMS) and totol harmonic distortion (THD) percentage of voltage and current generated by the inverter greatly determines the power quality of the inverter. This paper recount to analysis theorical and investigate the effect of different conduction modes on the power quality of a three-phase voltage source inverter. The design and employment of an Arduino based on the gate pulse generation technique to fire three-phase voltage source inverter's various conduction modes is also discussed. The firing of angles comprising of 120^0, 180^0, and 150^0 in conduction modes are comprised. The studies of various waveforms output voltage generated from various conduction modes, RMS voltage at fundamental frequencies, THD percentage are also included in this paper. Matlab/Simulink software has been employed in order to validate the proven of the theories. Moreover, this work, then verified through an experimental prototype setup based on Arduino implementation. Finally, the results of simulation are good argument with the experimental results.

Keywords: *Three-phase inverter, Conduction Mode, Fire of Angles, Arduino, THD*

1. INTRODUCTION

Recently, inverters have been employed on many applications, such as household, industry, military, renewable energy, transportation, aerospace and so on. Inverters are utilized to convert DC power from sources like solar panels, batteries, or fuel cells to AC power at desired voltage and frequency. In industrial applications, inverters have been engaged widely as Flexible AC Transmission System (FACTS) devices, Uninterruptible Power Supplies (UPS), Variable Frequency Drives (VFD), High Voltage Direct Current transmission system, Active Power Filters etc [1-4]. The inverter conversion can be accomplished either by controlled turn-on and turn-off power switches (e.g. BJTs, MOSFETs, IGBTs, and GTOs) or by forced commutated thyristors, rely on applications [5-11].

Generally, there were two types of inverter topology based on voltage and current source concept, named as Voltage Source Inverter (VSI) and Current Source Inverter (CSI). Voltage waveform is the independently controlled AC output in the VSI topologies. Meanwhile, in CSI topologies, the independently controlled AC output is a current waveform.

Based on output voltage phases, the inverter topology can be single-phase and three-phase inverter respectively. The single-phase inverter is commonly employed to low power applications. Meanwhile the three-phase inverter is applied to high power applications.

The output voltage of an inverter has a periodic waveform which is not purely sinusoidal, but with number of techniques it can be designed to closely approximate to this desired waveform. The output voltage waveforms can be sinusoidal wave, square-wave and quasi-wave. The sinusoidal waveform is an ideal voltage waveform of inverter. Nevertheless, a filter is needed for generating sinusoidal waveform. The sinusoidal signal reference in fundamental frequency is modulated in high frequency carrier. The sinusoidal waveform inverter is common operated to electric drives application. The square-wave and quasi-wave inverter can be employed to low and medium-power applications.

The triggering signals in an inverter are required to generate output voltage waveform. The frequency of triggering signal for power switching inverter can be low and high respectively. The sinusoidal waveform inverter is engaged to high frequency switching through sinusoidal pulse width modulation technique. The low frequency switching technique is employed to square-wave and quasi-wave inverter.

Many researchers have been conveyed concerning to employment of three-phase inverter for low frequency switching. The inverters can be conducted in 120^0, 150^0 and 180^0 for fundamental frequency. Design and implementation of Arduino based three-phase Inverter for 120^0 conduction mode has been reported [12], some aspects on three-phase inverter for 180^0 conduction mode has been explained [13], simulation three-phase inverter for only 120^0 and 180^0 conduction modes [14, 15] , simulation and experiment with low-cost processor ATMega8535 for only 120^0 and 180^0 conduction modes has been conducted [16], dynamic Voltage Restorer adopting 150^0 Conduction Angle VSI has been applied [17], Simulation three-phase VSI by 150 degree conduction has been reported [18], experimental circuit with Arduino circuit for 150^0 conduction mode has been applied [19], experimental circuit with PIC16F72 circuit from Microchip for 150^0 conduction mode has been applied [20], with PIC16F877A microcontroller has been done by [21, 22], simulation three-phase inverter for 120^0, 150^0 and 180^0 conduction mode has been done by[23-28] , design and implementation of a three-phase inverter operated with different conduction modes using ATMega microcontroller has been conducted by [29, 30]. Theoretical analysis of waveforms and odd harmonics of the voltage generated by a three-phase inverter with Fourier series representation is not yet available in the literature that discusses clearly and in detail.

This paper describes some theoretical, analytical and empirical issues of three-phase six switches quasi-square wave inverter for various conduction modes, namely 120^0, 150^0 and 180^0 conduction modes. Fourier series approach is employed to analyse the waveform and determine the magnitude of the harmonics generated from the various conduction modes applied to the three-phase inverter. The inverter was designed, fabricated, and tested by considering load as a resistive. The algorithmic rules of all firing angles for power switching are enclosed in a low-cost processor Adruino Uno 328.

2. STRUCTURE OF TOPOLOGY

In the all industrial application variable frequency & voltage require for different application. Three-phase six-switch bridge inverter is more popular than any other inverter topology. A three-phase inverter may be viewed as three single-phase inverters and the output of each single phase is shifted by 120˚ with respect to each other. A Three phase inverter can be constructed by combining three single phase half bridge inverters as shown in Figure 1, where S_1 S_2, S_3, S_4, S_5 and S_6 are the power switches and A, B, and C are phase sequence respectively. It consists of six power switches with six associated with freewheeling diodes. The switches are opened and closed periodically in the proper sequence to produce the desired output waveform. The output from this inverter is to be fed to a three-phase balanced resistor load. The switching signals for each inverter leg are displaced by 120^0 with respect to the adjacent legs. The output line-line voltages are determined by the potential differences between the output terminals of each leg.

There are three conduction modes of gating power switches for three-phase inverter. They are 180^0, 150^0, and 120^0 conduction modes. Six-step operation is needed to generate waveform in one cycle for 180^0 and 120^0 conduction modes. Meanwhile, 150^0 conduction mode requires twelve-step operation for one cycle output voltage waveform.

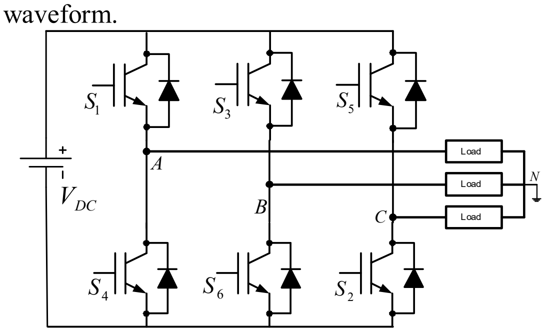

Figure 1: The Three-phase Inverter Topology

2.1 180^0 Conduction Mode

In this case, each switch is turned ON for 180^0. Power switches S_1 and S_4, which belong to the left-most inverter leg, produces the output voltage for phase A. The switching signals for S_1 and S_4 are complementary, as are for S_3 and S_6 or S_5 and S_2. The switching signals for switches S_3 and S_6, (which are for phase *B*, belonging to the middle leg), are delayed by 120^0 from those for S_1 and S_4 respectively, for the *A-B-C* phase sequence. Similarly, for the same phase sequence, the switching signals for switches S_5 and S_2 are delayed from the switching signals for S_3 and S_6 by 120^0.

ISSN: 1992-8645 www.jatit.org E-ISSN: 1817-3195

The phase terminal voltages at A, B and C are determined by the states of the switches connected at each pole. Note that with 180^0 conduction mode, each pole voltage can have only two values, namely $+(1/2)V_{DC}$ or $-(1/2)V_{DC}$

In 180^0 conduction modes of the operation, three are six-state operation modes, each state is operated during 60^0. There are three power switches that conduct at each-step operation. Operation of switches in 180° conduction modes is shown in Table 1.

The line-line voltages, V_{AB}, V_{BC} and V_{CA} are determined from the switching states at the poles and the DC source voltage, (V_{DC}). Thus, when switches S_1 and S_3 are ON, V_{AB} = 0V, when S_1 and S_6 are ON, $V_{AB} = +V_{DC}$, and so on. The line-line voltages V_{AB}, V_{BC} and V_{CA} are therefore quasi-square waveforms of 120^0 of ON and 60^0 of OFF durations.

Line-neutral voltages are determined from the switching states and the neutral point voltage of the load which can be found by assuming that the load consists of a balanced three-phase resistor bank. For instance, if S_1, S_3 and S_2 are ON, the potential of the neutral point of the load is $+(2/3)V_{DC}$ and therefore V_{AN} and V_{BN} will each be at potentials $+(1/3)V_{DC}$ while V_{CN} will be at $-(2/3)V_{DC}$. Similarly, when S_4, S_2 and S_3 are ON, the potential of the neutral point will be $+(1/3)V_{DC}$. As a result, the potential V_{BN} will become $+(2/3)V_{DC}$ and V_{AN} and V_{CN} will each be at $(1/3)V_{DC}$.

The line-line output voltages are obtained by subtracting two square-wave waveforms which are 120^0 displaced from each other. Each of these waveforms would consist of harmonics orders 1, 3, 5, 7, 9, … and so on. Because of the 120^0 phase shift between the waveforms, the triplen harmonics (of order which are multiples of 3) of both will of the same phase and hence these cancel in the process of subtraction. Consequently, the triplen order harmonic voltages are eliminated from the line–line voltage. The remaining harmonics are at $n = 6r \pm 1$where r is any positive integer, the n^{th} harmonic having an amplitude $1/n$ times the fundamental component.

The line-line quasi-square output voltage waveform of Figure 2 has amplitude V_{DC} and duration $\delta = 120^0$.

Fourier series representation of this waveform is

$$V_{l-l} = \sum_{n=1,3,5,..}^{\infty} \frac{4V_{DC}}{n\pi} \sin\left(\frac{n\delta}{2}\right) \cos n\omega_0 t \quad (1)$$

$$V_{l-l} = \frac{2\sqrt{3}}{\pi} V_{DC} \left[\cos(\omega_0 t) + \frac{1}{5}\cos(5\omega_0 t) + \frac{1}{7}\cos(7\omega_0 t) + \frac{1}{11}\cos(11\omega_0 t) + \cdots\right] \quad (2)$$

$$V_{l-l,1} = \frac{2\sqrt{3}}{\pi} V_{DC} \ ; \ V_{l-l,5} = \frac{2\sqrt{3}}{5\pi} V_{DC};$$

$$V_{l-l,7} = \frac{2\sqrt{3}}{7\pi} V_{DC} \ ; V_{l-l,11} = \frac{2\sqrt{3}}{11\pi} V_{DC}; \quad (3)$$

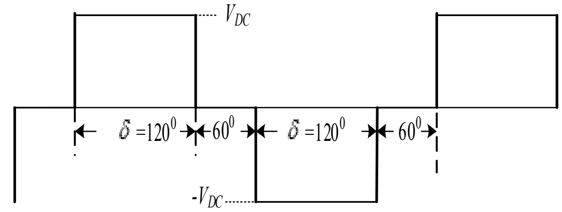

Figure 2: The Line-line Voltage Waveform of 180^0 Conduction Mode

The RMS value of the fundamental and higher order output voltages are : Thus the fundamental RMS output, $V_{l-l,1} = 0.78V_{DC}$. The line-neutral voltage waveform for this inverter is as shown in Figure 3. Fourier series representation of this waveform is given by

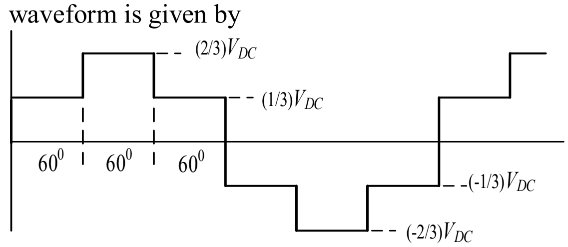

Figure 3: The Line-neutral Voltage Waveform of 180^0 Conduction Mode

Table 1: Operation of Switches in 180^0 Conduction Modes.

State	Duration	Switching state						Output Voltage					
		S_1	S_2	S_3	S_4	S_5	S_6	V_{ab}	V_{bc}	V_{ca}	V_{an}	V_{bn}	V_{cn}
1	π/3	1	0	0	0	1	1	V_{DC}	$-V_{DC}$	0	$1/3V_{DC}$	$-2/3V_{DC}$	$1/3V_{DC}$
2	π/3	1	1	0	0	0	1	V_{DC}	0	$-V_{DC}$	$2/3V_{DC}$	$-1/3V_{DC}$	$-1/3V_{DC}$
3	π/3	1	1	1	0	0	0	0	V_{DC}	$-V_{DC}$	$1/3V_{DC}$	$1/3V_{DC}$	$-2/3V_{DC}$
4	π/3	0	1	1	1	0	0	$-V_{DC}$	V_{DC}	0	$-1/3V_{DC}$	$2/3V_{DC}$	$-1/3V_{DC}$
5	π/3	0	0	1	1	1	0	$-V_{DC}$	0	V_{DC}	$-2/3V_{DC}$	$1/3V_{DC}$	$1/3V_{DC}$
6	π/3	0	0	0	1	1	1	0	$-V_{DC}$	V_{DC}	$-1/3V_{DC}$	$-1/3V_{DC}$	$2/3V_{DC}$

ISSN: 1992-8645 www.jatit.org E-ISSN: 1817-3195

$$V_{l-n} = \sum_{n=1,3,5,..}^{\infty} \frac{4V_{DC}}{n\pi} \sin\left(\frac{n\delta}{2}\right) \cos n\omega_0 t \quad (4)$$

$$V_{l-n} = \sum_{n=1,3,5,..}^{\infty} \left[\frac{4V_{DC}}{3n\pi} \sin\left(\frac{n\pi}{2}\right) + \frac{4V_{DC}}{3n\pi} \sin\left(\frac{n\pi/3}{2}\right)\right] \cos n\omega_0 t \quad (5)$$

$$V_{l-n} = \frac{2}{\pi} V_{DC} \left[\cos(\omega_0 t) + \frac{1}{5}\cos(5\omega_0 t) + \frac{1}{7}\cos(7\omega_0 t) + \frac{1}{11}\cos(11\omega_0 t) + \cdots\right] \quad (6)$$

$$V_{l-n,1} = \frac{2}{\pi} V_{DC}\ ; V_{l-n,5} = \frac{2}{5\pi} V_{DC};$$
$$V_{l-n,7} = \frac{2}{7\pi} V_{DC}\ ; V_{l-n,11} = \frac{2}{11\pi} V_{DC}; \quad (7)$$

RMS values of the fundamental and higher order terms of the line-neutral voltage are:

$$V_{l-n,1} \approx \frac{\sqrt{2}}{\pi} V_{DC} \quad (8)$$

2.2 120^0 Conduction Mode

In this conduction mode each switch conducts for 120°-time period or 2π/3 radians. At any instant of time, two switches will conduct simultaneously. After every 60° or π/3 radians, one of the conducting switches is turned off and some other switch will start conducting. There is a delay of π/3 between turning on and turning off of switches of same leg. So there is no possibility of short circuit. Operation of switches in 120° conduction modes is shown in Table 2.

The line-line voltage waveform for this inverter is as shown in Figure 4. Fourier series representation of this waveform is given by

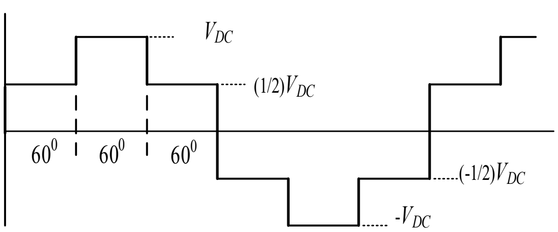

Figure 4: The Line-line Voltage Waveform of 120^0 Conduction Mode

$$V_{l-l} = \sum_{n=1,3,5,..}^{\infty} \frac{4V_{DC}}{n\pi} \sin\left(\frac{n\delta}{2}\right) \cos n\omega_0 t \quad (9)$$

$$V_{l-l} = \sum_{n=1,3,5,..}^{\infty} \left[\frac{4V_{DC}}{2n\pi} \sin\left(\frac{n\pi}{2}\right) + \frac{4V_{DC}}{2n\pi} \sin\left(\frac{n\pi/3}{2}\right)\right] \cos n\omega_0 t \quad (10)$$

$$V_{l-l} = \frac{3}{\pi} V_{DC} \left[\cos(\omega_0 t) + \frac{1}{5}\cos(5\omega_0 t) + \frac{1}{7}\cos(7\omega_0 t) + \frac{1}{11}\cos(11\omega_0 t) + \cdots\right] \quad (11)$$

$$V_{l-l,1} = \frac{3}{\pi} V_{DC};\ V_{l-l,5} = \frac{3}{5\pi} V_{DC}\ ;$$
$$V_{l-l,7} = \frac{3}{7\pi} V_{DC}\ ; V_{l-l,11} = \frac{3}{11\pi} V_{DC}.. \quad (12)$$

Thus the fundamental RMS output, $V_{l-l,1} \approx 0.69V_{DC}$

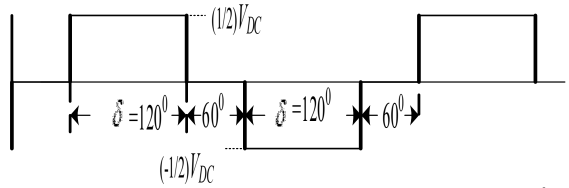

Figure 5: The Line-neutral Voltage Waveform of 120^0 Conduction Mode

The line-line quasi-square output voltage waveform of Figure 5 has amplitude $(1/2)V_{DC}$ and duration δ = 120^0. Fourier series representation of this waveform is given by

$$V_{l-n} = \sum_{n=1,3,5,..}^{\infty} \frac{4V_{DC}}{2n\pi} \sin\left(\frac{n\delta}{2}\right) \cos n\omega_0 t \quad (13)$$

$$V_{l-n} = \frac{\sqrt{3}}{\pi} V_{DC} \left[\cos(\omega_0 t) + \frac{1}{5}\cos(5\omega_0 t) + \frac{1}{7}\cos(7\omega_0 t) + \frac{1}{11}\cos(11\omega_0 t) + \cdots\right] \quad (14)$$

The amplitude value of the fundamental and higher order output line-neutral voltages are thus,

$$V_{l-n,1} = \frac{\sqrt{3}}{\pi} V_{DC};\ V_{l-n,5} = \frac{\sqrt{3}}{5\pi} V_{DC}\ ;$$
$$V_{l-n,7} = \frac{\sqrt{3}}{7\pi} V_{DC}\ ; V_{l-n,11} = \frac{\sqrt{3}}{11\pi} V_{DC}.... \quad (15)$$

Therefore RMS value of output line-neutral voltage is $V_{l-n,1} \approx 0.40V_{DC}$.

The amplitude value of the fundamental and higher order output line-neutral voltages are thus,

$$V_{l-n,1} = \frac{\sqrt{3}}{\pi} V_{DC};\ V_{l-n,5} = \frac{\sqrt{3}}{5\pi} V_{DC}\ ;$$
$$V_{l-n,7} = \frac{\sqrt{3}}{7\pi} V_{DC}\ ; V_{l-n,11} = \frac{\sqrt{3}}{11\pi} V_{DC}.... \quad (15)$$

Therefore RMS value of output line-neutral voltage is $V_{l-n,1} \approx 0.40V_{DC}$.

ISSN: 1992-8645 www.jatit.org E-ISSN: 1817-3195

Table 2: Operation of Switches In 120⁰ Conduction Modes.

State	time	Switching state						Output Voltage					
		S_1	S_2	S_3	S_4	S_5	S_6	V_{ab}	V_{bc}	V_{ca}	V_{an}	V_{bn}	V_{cn}
1	π/3	1	0	0	0	0	1	V_{DC}	-1/2V_{DC}	-1/2V_{DC}	1/2V_{DC}	-1/2V_{DC}	0
2	π/3	1	1	0	0	0	0	1/2V_{DC}	1/2V_{DC}	-V_{DC}	1/2V_{DC}	0	-1/2V_{DC}
3	π/3	0	1	1	0	0	0	-1/2V_{DC}	V_{DC}	-1/2V_{DC}	0	1/2V_{DC}	-1/2V_{DC}
4	π/3	0	0	1	1	0	0	-V_{DC}	1/2V_{DC}	1/2V_{DC}	-1/2V_{DC}	1/2V_{DC}	0
5	π/3	0	0	0	1	1	0	-1/2V_{DC}	-1/2V_{DC}	V_{DC}	-1/2V_{DC}	0	1/2V_{DC}
6	π/3	0	0	0	0	1	1	1/2V_{DC}	-V_{DC}	1/2V_{DC}	0	-1/2V_{DC}	2/2V_{DC}

2.3 150⁰ Conduction Mode

For 150° conduction mode, each power switches conducts for 150° of a cycle. For completing one cycle of the output ac voltage unlike 180° mode & 120° mode inverter, 150° has twelve steps with each of 30° durations. The switching patterns are presented per cycle with each pattern duration is 30°. These transistors conduct in one interval, while only two transistors conduct in the next one, as in 180° and 120° conduction modes respectively. Operation of switches in 150° conduction modes is shown in Table 3.

The line-line quasi-square output voltage waveform of Figure 6 has amplitude V_{DC} and duration δ = 150⁰.

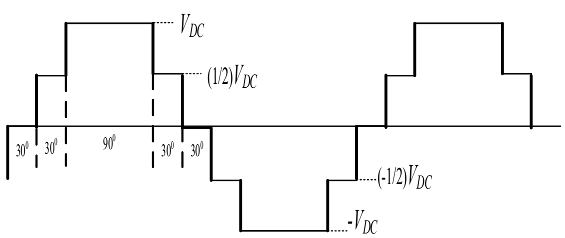

Figure 6: The Line-line Voltage Waveform of 150⁰ Conduction Mode

Fourier series representation of this waveform is

$$V_{l-l} = \sum_{n=1,3,5,..}^{\infty} \frac{4V_{DC}}{n\pi} \sin\left(\frac{n\delta}{2}\right) \cos n\omega_0 t \quad (16)$$

$$V_{l-l} = \sum_{n=1,3,5,..}^{\infty} \left[\frac{4V_{DC}}{2n\pi} \sin\left(\frac{n5\pi/6}{2}\right) + \frac{4V_{DC}}{2n\pi} \sin\left(\frac{n\pi/4}{2}\right)\right] \cos n\omega_0 t \quad (16)$$

$$V_{l-l} = \frac{2\sqrt{3}}{\pi} V_{DC} \left[\cos(\omega_0 t) + \frac{1}{5}\cos(5\omega_0 t) + \frac{1}{7}\cos(7\omega_0 t) + \frac{1}{11}\cos(11\omega_0 t) + \cdots\right] \quad (17)$$

The value of the fundamental and higher order output voltages are:

$$V_{l-n,1} = \frac{2\sqrt{3}}{\pi} V_{DC}\ ;\ V_{l-n,5} = \frac{2\sqrt{3}}{5\pi} V_{DC};$$

$$V_{l-n,7} = \frac{2\sqrt{3}}{7\pi} V_{DC}\ ; V_{l-n,11} = \frac{2\sqrt{3}}{11\pi} V_{DC}; \quad (18)$$

Thus the fundamental RMS output,
$V_{l-l,1} = 0.78V_{DC}$

The line-neutral voltage waveform for this inverter is as shown in Figure 7. Fourier series representation of this waveform is given by

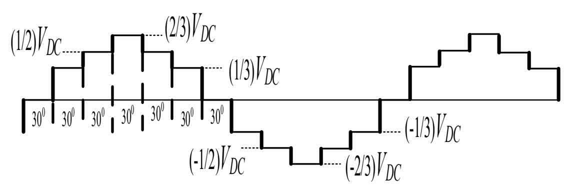

Figure 7: The Line-neutral Voltage Waveform of 150⁰ Conduction Mode

$$V_{l-n} = \sum_{n=1,3,5,..}^{\infty} \frac{4V_{DC}}{n\pi} \sin\left(\frac{n\delta}{2}\right) \cos n\omega_0 t \quad (19)$$

$$V_{l-n} = \sum_{n=1,3,5,..}^{\infty} \left[\frac{4V_{DC}}{3n\pi} \sin\left(\frac{n\pi}{2}\right) + \frac{4V_{DC}}{3n\pi} \sin\left(\frac{n\pi/3}{2}\right)\right] \cos n\omega_0 t \quad (20)$$

$$V_{l-n} = \frac{2}{\pi} V_{DC} \left[\cos(\omega_0 t) + \frac{1}{5}\cos(5\omega_0 t) + \frac{1}{7}\cos(7\omega_0 t) + \frac{1}{11}\cos(11\omega_0 t) + \cdots\right] \quad (21)$$

$$V_{l-n,1} = \frac{2}{\pi} V_{DC}\ ;\ V_{l-n,5} = \frac{2}{5\pi} V_{DC};$$

$$V_{l-n,7} = \frac{2}{7\pi} V_{DC}\ ; V_{l-n,11} = \frac{2}{11\pi} V_{DC}; \quad (22)$$

RMS values of the fundamental and higher order terms of the line-neutral voltage are:

$$V_{l-n,1} \approx \frac{\sqrt{2}}{\pi} V_{DC} \quad (23)$$

Table 3. Switching States for 150° Conduction Mode

ISSN: 1992-8645 www.jatit.org E-ISSN: 1817-3195

State	time	Switching state						Output Voltage					
		S_1	S_2	S_3	S_4	S_5	S_6	V_{ab}	V_{bc}	V_{ca}	V_{an}	V_{bn}	V_{cn}
1	$\pi/6$	1	0	0	0	0	0	0	V_{DC}	$-V_{DC}$	$1/3V_{DC}$	$1/3V_{DC}$	$-2/3V_{DC}$
2	$\pi/6$	1	1	0	0	0	0	$-1/2V_{DC}$	V_{DC}	$-1/2V_{DC}$	0	$1/2V_{DC}$	$-1/2V_{DC}$
3	$\pi/6$	1	1	1	0	0	0	$-V_{DC}$	V_{DC}	0	$-1/3V_{DC}$	$2/3V_{DC}$	$-1/3V_{DC}$
4	$\pi/6$	1	1	1	1	0	0	$-V_{DC}$	$1/2V_{DC}$	$1/2V_{DC}$	$-1/2V_{DC}$	$1/2V_{DC}$	0
5	$\pi/6$	1	1	1	1	1	0	$-V_{DC}$	0	V_{DC}	$-2/3V_{DC}$	$1/3V_{DC}$	$1/3V_{DC}$
6	$\pi/6$	0	1	1	1	1	1	$-1/2V_{DC}$	$-1/2V_{DC}$	V_{DC}	$-1/2V_{DC}$	0	$1/2V_{DC}$
7	$\pi/6$	0	0	1	1	1	1	0	$-V_{DC}$	V_{DC}	$-1/3V_{DC}$	$-1/3V_{DC}$	$2/3V_{DC}$
8	$\pi/6$	0	0	0	1	1	1	$1/2V_{DC}$	V_{DC}	$1/2V_{DC}$	0	$-1/2V_{DC}$	$1/2V_{DC}$
9	$\pi/6$	0	0	0	0	1	1	V_{DC}	$-V_{DC}$	0	$1/3V_{DC}$	$-2/3V_{DC}$	$1/3V_{DC}$
10	$\pi/6$	0	0	0	0	0	1	V_{DC}	$-1/2V_{DC}$	$-1/2V_{DC}$	$1/2V_{DC}$	$-1/2V_{DC}$	0
11	$\pi/6$	0	0	0	0	0	0	V_{DC}	0	$-V_{DC}$	$2/3V_{DC}$	$-1/3V_{DC}$	$-1/3V_{DC}$
12	$\pi/6$	0	0	0	0	0	0	$1/2V_{DC}$	$1/2V_{DC}$	$-V_{DC}$	$1/2V_{DC}$	0	$-1/2V_{DC}$

2.4. Arduino Uno and Inverter Circuits

In this proposed scheme, the conduction mode algorithmes for generating output waveform is embedded in a low processor Arduino Uno board. The Arduino Uno is a microcontroller board depending on the ATmega328. It includes 14 digital input/output pins (out of which 6 can be exploited as PWM outputs), 6 analog inputs, a 16 MHz crystal oscillator, a USB connection, a power jack, an ICSP header and the last one is a reset button. It includes the most necessary things which are essential to support the microcontroller; basically attach it to a computer with a USB cable or power it with an AC-to-DC adapter or battery to get started.

The six-signals is produced by microcontroller is fed to gate drive circuits. The gate drive circuits is employed to isolate power switching circuit of inverter with controlling circuit from microcontroller and also to boost input signal from 5V be 15V. The IGBT power switches is be trigger with ±15V. The inverter is connected to gate drive circuits. This illustration can be shown in Figure 8.

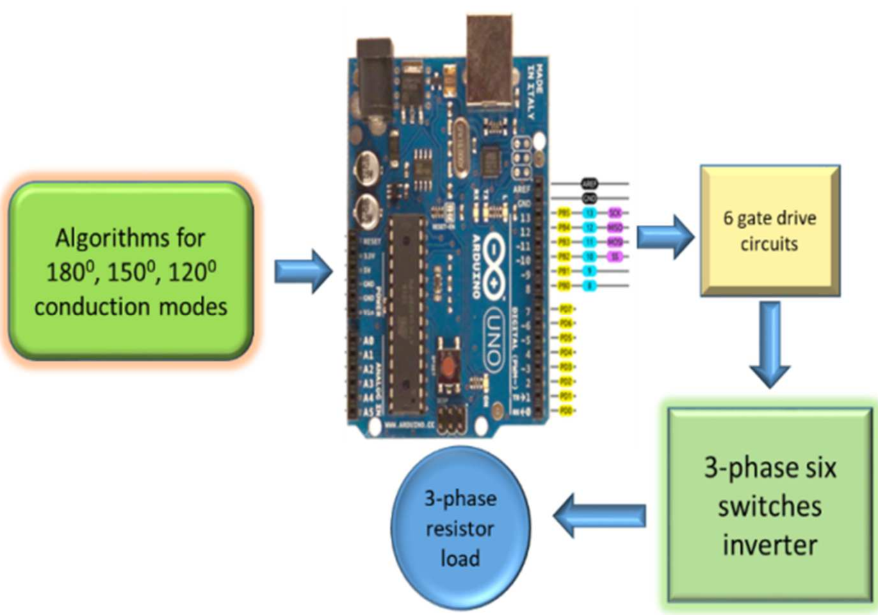

Figure 8: The Proposed Schema of Three-phase Inverter

Journal of Theoretical and Applied Information Technology
15th April 2022. Vol.100. No 7

ISSN: 1992-8645 www.jatit.org E-ISSN: 1817-3195

3. SIMULATION AND EXPERIMENT RESULT

In order to prove the efficacy of the inverter designed, the simulation and experimental environment was tested to see performance of the inverter. The output voltage from the inverter and THD were observed, the proposed scheme was tested in different conduction modes. The proposed scheme inverter was simulated and tested at the frequency of 50 Hz using Simulink/Matlab software. The input DC voltage of the inverter used was 100V, the power switches of six-G4PH50UD were used meanwhile a three-phase of 100Ω resistor was used as a load.

The performance of the inverter was measured using PINTEK DP-25 (a high voltage differential probe), GwINSTEK GDS-2074A (4-channel digital oscilloscope) and KYORISU (three-phase power quality analyser). The configuration of a three-phase inverter for simulation and experimental setup can be shown in Figure 9.

3.1. The Conduction Mode 180^0

Figure 10 to Figure 14 which are left side of the results of simulation meanwhile the experimental results can be observed on the right side. All the results of simulation and experiments were conducted in mode conduction in 180^0. The gating signal in the cases of the switches of S_1, S_2 and S_3 can be illustrated in Fig. 10 meanwhile the gating signal of the switches of S_4, S_5 and S_6 can be observed in Figure 11. By the way each power switch is turned-on in every π radian. Consequently, the phase output of voltage ($V_{l\text{-}n}$) contains four DC level voltages meanwhile the line output of the voltage ($V_{l\text{-}l}$) is only has three level DC voltage, as presented in Figure 12 and Figure 13, respectively. In this conduction mode, the generated harmonic distortion of line-line or line-neutral output voltage achieve roughly 30%, while RMS line-line output voltage reach 80V and line-neutral output voltage in fundamental frequency is 63V as shown in Figure 14.

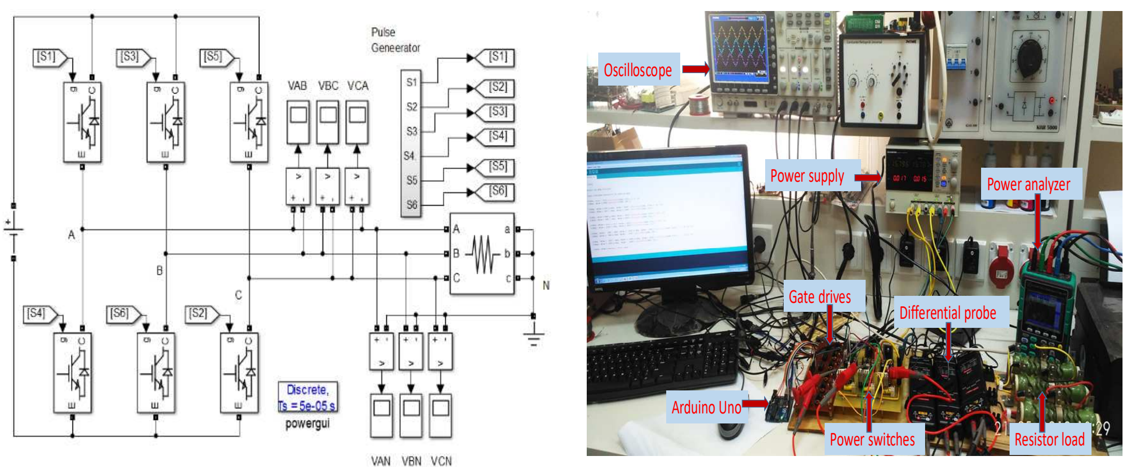

(a) (b)

Figure 9: The Configuration Three-phase Inverter (a) Simulation, (b) Experiment Set-up

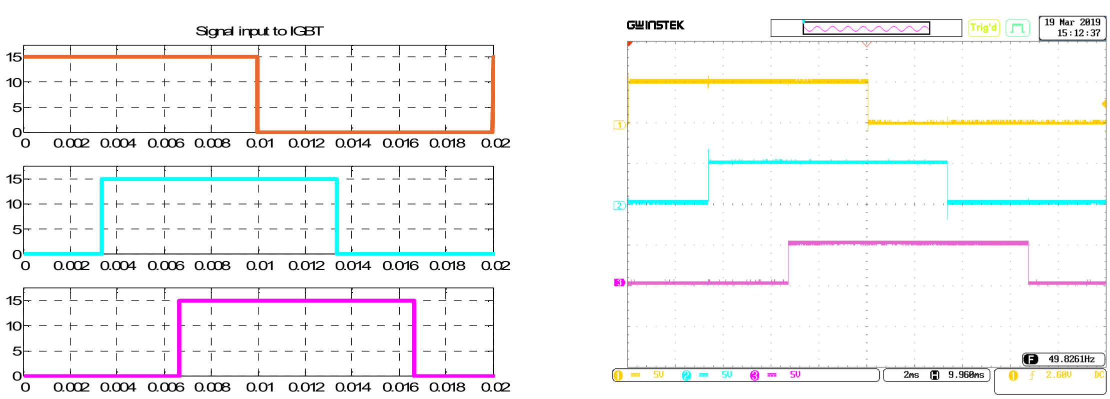

(a) (b)

Figure 10: The Switching Signal of S_1, S_3, S_5 (a) Simulation, (b) Experiment for the Conduction Mode 180^0

Journal of Theoretical and Applied Information Technology
15th April 2022. Vol.100. No 7

ISSN: 1992-8645 www.jatit.org E-ISSN: 1817-3195

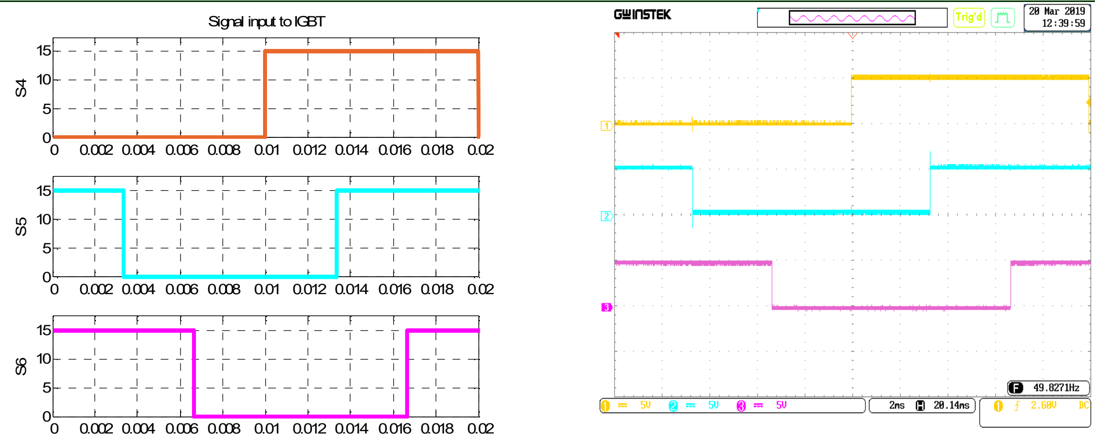

(a) (b)

Figure 11: The Switching Signal of S_2, S_4, S_6 (a) Simulation, (b) Experiment for the Conduction Mode 180⁰

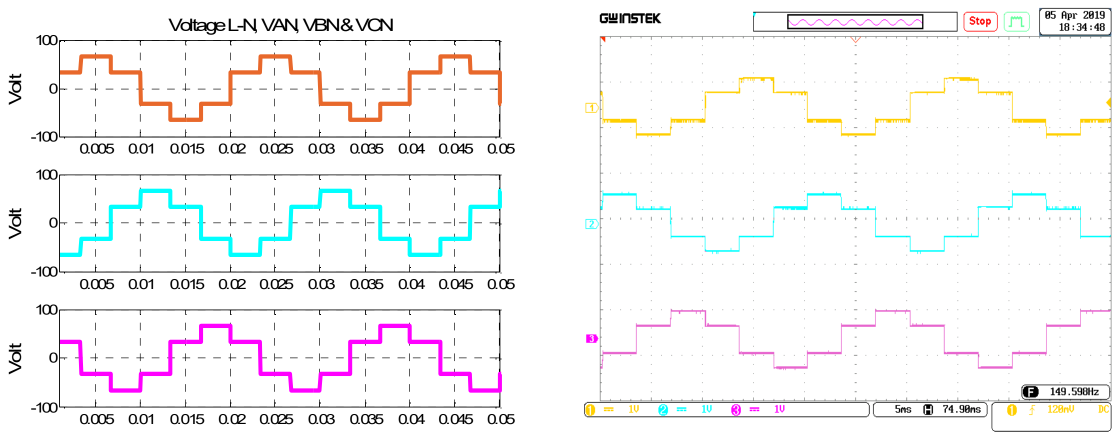

(a) (b)

Figure 12: The Output Voltage Waveform (V_{L-N}) (a) Simulation, (b) Experiment for the Conduction Mode 180⁰

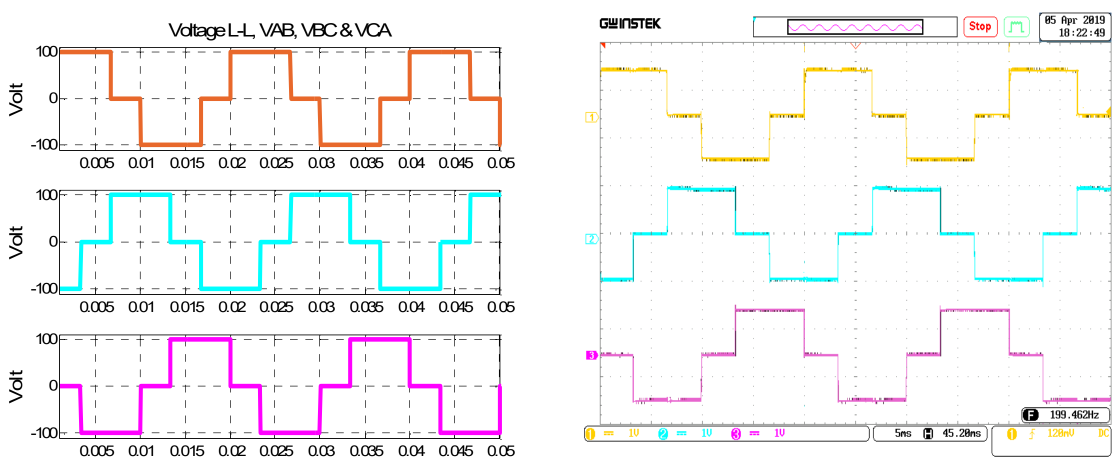

(a) (b)

Figure 13: The Output Voltage Waveform (V_{L-L}) (a) Simulation, (b) Experiment for the Conduction Mode 180⁰

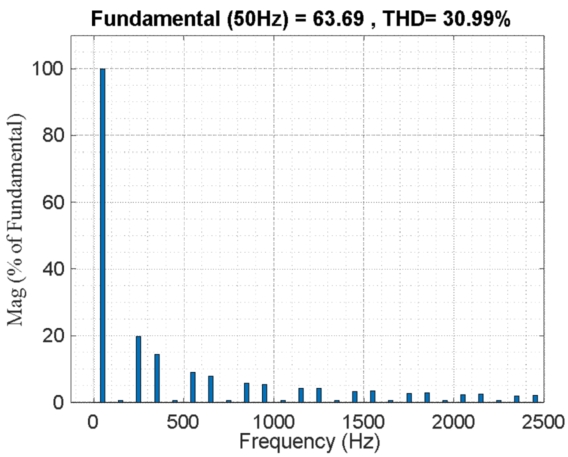

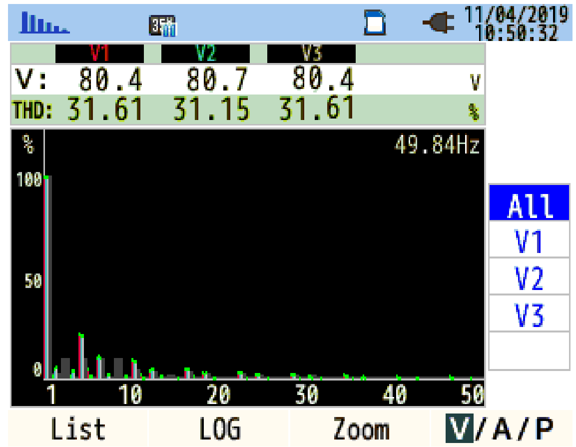

(a) (b)

Figure 14: The FFT Analysis on V_{L-N} (a) Simulation, (b) Experiment for the Conduction Mode 180^0

3.2. 120-degree Conduction Mode

Figure-15 shows the experiment result of the gating signals S_1, S_2 and S_3 for 120^0 conduction mode meanwhile the gating signals S_4, S_5 and S_6 are shown in Figure-16. In those figures, two power switches are ON every π/3 radian. Each power switches conducts every (2/3) π. In this conduction mode, the phase voltage output (V_{l-n}) generates the 3 voltage levels and the maximum level V_{DC} used reaches 50% of V_{Dc}. Meanwhile, the line voltage outputs (V_{l-l}) generate 4 voltage levels and the used level maximum V_{DC} archives 100% of V_{Dc}. Those are shown in Figure 17 and Figure 18, respectively. The FFT analysis on V_{l-n} with Simulink/Matlab and experimental results indicate the same values. The harmonic distortion of output voltage for 120^0 conduction mode reach 31% as shown in Figure 19.

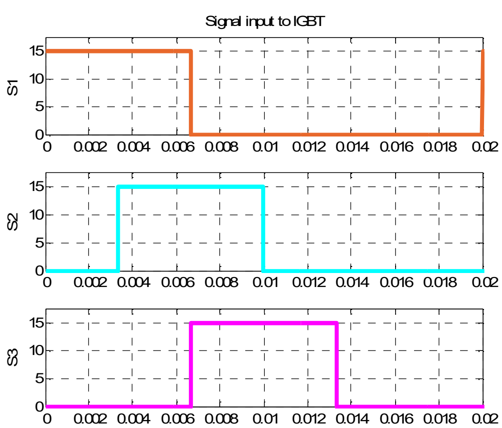

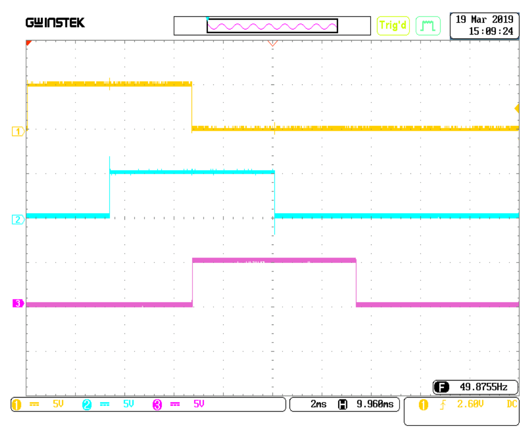

(a) (b)

Figure 15: The Switching Signal of S_1, S_2, S_3 (a) Simulation, (b) Experiment for the Conduction Mode 120^0

ISSN: 1992-8645 www.jatit.org E-ISSN: 1817-3195

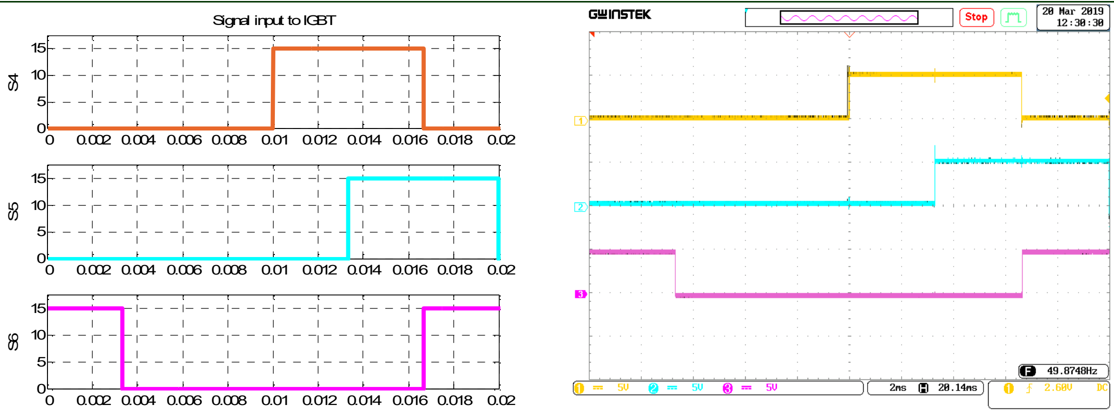

(a) (b)

Figure 16: The Switching Signal of S_4, S_5, S_6 (a) Simulation, (b) Experiment for the Conduction Mode 120^0

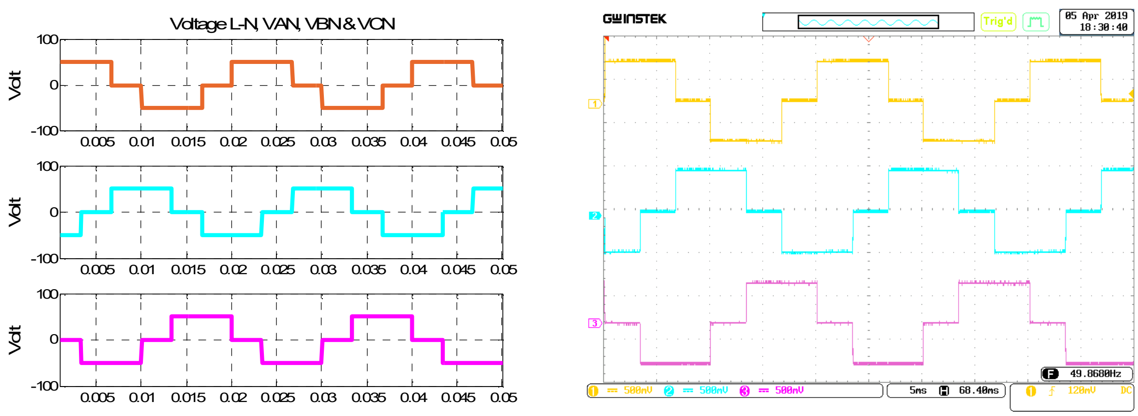

(a) (b)

Figure 17: The Output Voltage Waveform (V_{L-N}) (a) Simulation, (b) Experiment for the Conduction Mode 120^0

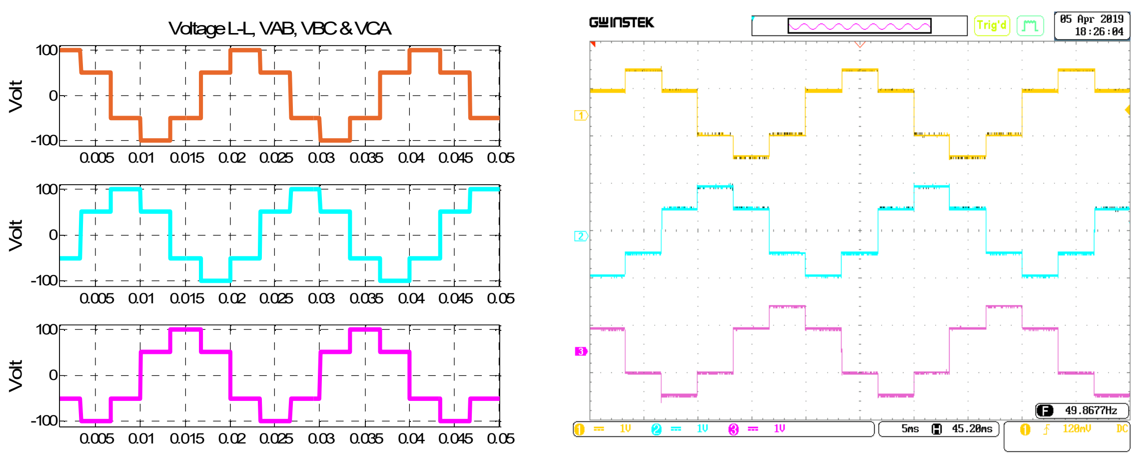

(a) (b)

Figure 18: The Output Voltage Waveform (V_{L-L}) (a) Simulation, (b) Experiment for the Conduction Mode 120^0

Journal of Theoretical and Applied Information Technology
15th April 2022. Vol.100. No 7

ISSN: 1992-8645 www.jatit.org E-ISSN: 1817-3195

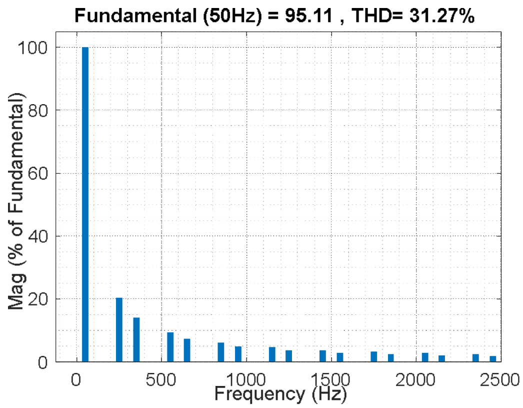

(a)

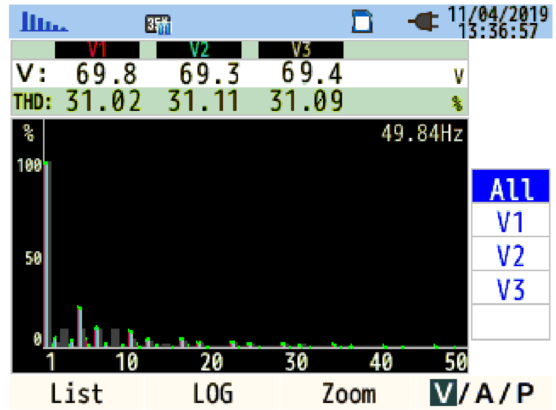

(b)

Figure 19: The FFT Analysis on V_{L-N} (a) Simulation, (b) Experiment for the Conduction Mode 120⁰

3.3. 150-degree Conduction Mode

In this conduction mode, each switch is conduct for 150°, means its duty cycle is 41.67%. The 12 switching patterns with 30^0 durations are formed in this mode. The switching pattern S_1, S_2, S_3, S_4, S_5 and S_6 for this conduction mode is shown in Figure 20 and Figure 21 respectively. The 150° conduction mode has more levels than 120^0 and 180^0 conduction modes and also the output voltage waveforms are symmetrical and contain zero as one level so it will reduce the harmonics. In Figure 22, the output phase voltage (V_{l-n}) develops to be 7 levels, 12 steps waveform. Meanwhile, the line voltage (V_{l-l}) becomes 5 levels are shown in Figure 23. As output voltage waveform approaches sinusoidal waveform, therefore THD of this conduction mode is reduced. It is achieved 16.8% as shown in Figure 24.

The output voltage waveform can be improved by using the 150^0 conduction mode, which is closer to a sinusoidal waveform. In 150^0 conduction mode, the RMS output voltage is almost identical to that in 180^0 conduction mode.

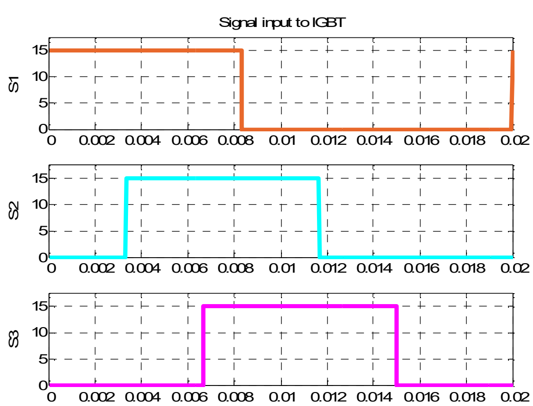

(a)

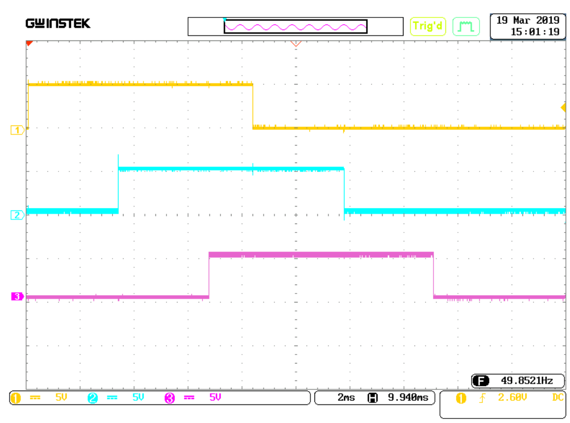

(b)

Figure 20: The Switching Signal of S_1, S_2, S_3 (a) Simulation, (b) Experiment for the Conduction Mode 150^0

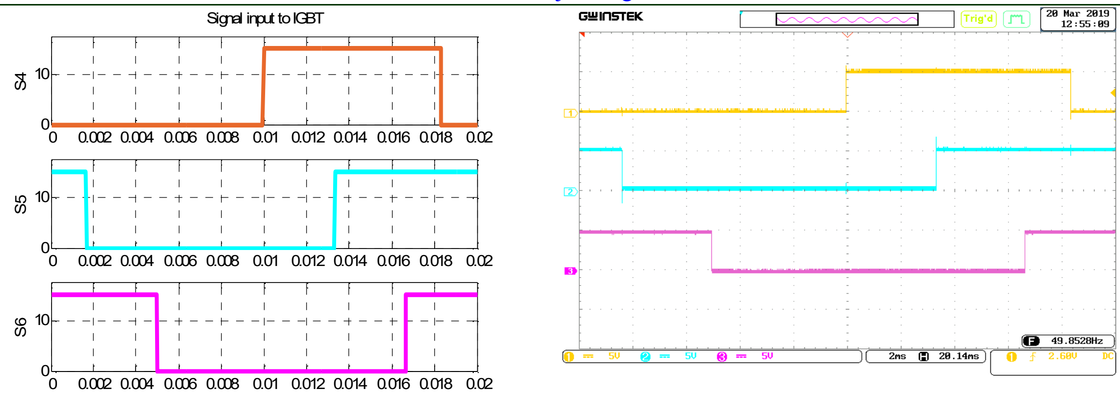

(a) (b)

Figure 21: The Switching Signal of S_4, S_5, S_6 (a) Simulation, (b) Experiment for the Conduction Mode 150^0

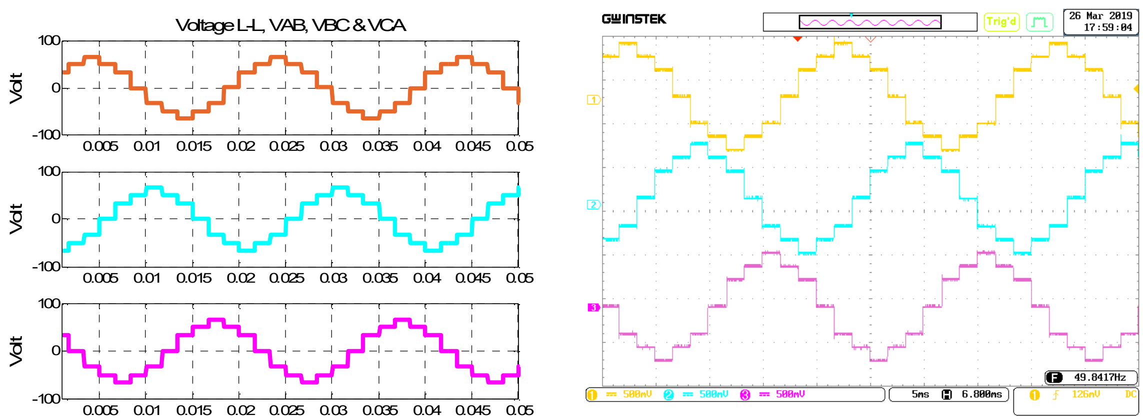

(a) (b)

Figure 22: The Output Voltage Waveform (V_{L-N}) (a) Simulation, (b) Experiment for the Conduction Mode 150^0

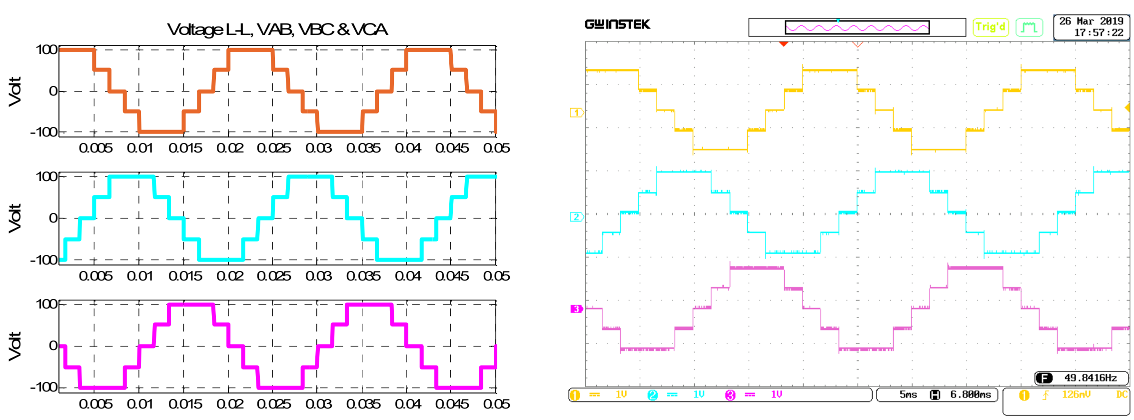

(a) (b)

Figure 23: The Output Voltage Waveform (V_{L-L}) (a) Simulation, (b) Experiment for the Conduction Mode 150^0

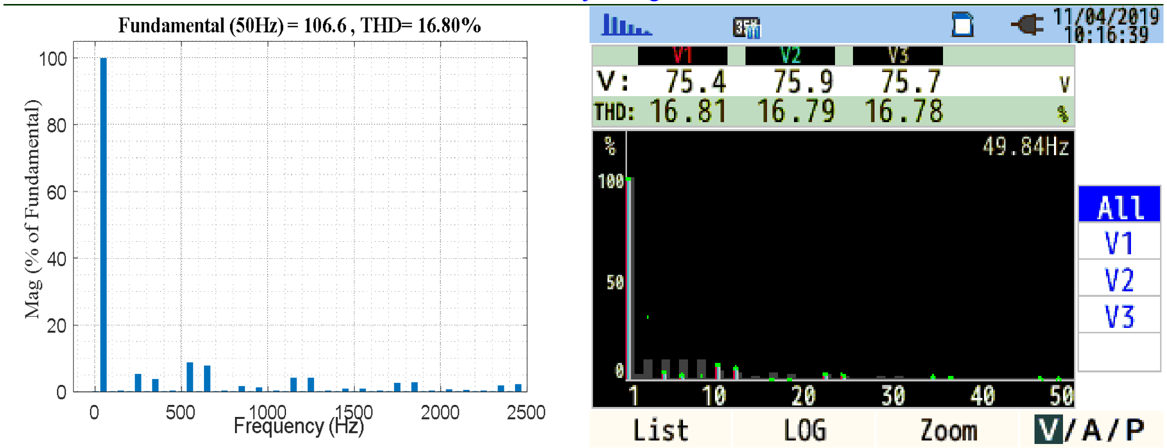

(a) (b)

Figure 24: The FFT Analysis on V_{L-N} (a) Simulation, (b) Experiment for the Conduction Mode 150^0

4. CONCLUSION

This paper presented a detail analysis the various conduction modes of three-phase inverter namely 180°, 120°, and 150°. A low cost microcontroller board such as Arduino Uno has been employed to generate pulse for six-switch three-phase voltage source inverter in various conduction modes. Low switching frequency program algorithms with 120^0, 150^0 and 180^0 conduction mode were embedded in the microcontroller target board. The features to evaluate different modes are described, criteria for selecting distinct various modes are presented, and simulation and experiment results demonstrate the analyses reliability.

ACKNOWLEDGEMENTS

Authors gratefully acknowledge the support of the Kementerian Riset, Teknologi, and Pendidikan Tinggi of Republic Indonesia and LP2M Universitas Negeri Padang under Penelitian Terapan Perguruan Tinggi Scheme. Project No. 945/UN35.136/LT/2021.

REFERENCES:

[1] R. Shah, D. Shah, P. Shah, and S. Thakur, "Simulation and Analysis of 150° Conduction Mode For Three Phase Voltage Source Inverter " presented at the *Recent trends in Electrical and Electronics & Communication Engineering (RTEECE) Conference*, 8th-9th April 2016, India, 2016.

[2] K. Vengadakrishnan, N. Madhanakkumar, P. Pugazhendiran, C. Bharatiraja, and V. Sriramkumar, "Torque ripple minimization of PMBLDC motor using simple boost inverter," *International Journal of Power Electronics Drive Systems (IJPEDS),* vol. 10, no. 4, pp. 1714-1723, 2019.

[3] M. Hasoun, A. El Afia, M. Khafallah, and K. Benkirane, "Field oriented control based on a 24-sector vector space decomposition for dual three-phase PMSM applied on electric ship propulsion," *International Journal of Power Electronics (IJPEDS),* vol. 11, no. 3, pp. 1175-1187, 2020.

[4] A. Iqbal and S. Moinuddin, "Assessment of torque pulsation in inverter fed three-phase induction motor drive for 180° and 150° conduction modes*"*. 2008, pp. 323-328.

[5] G. Rajpriya, S. Ravi, and A. M. A. Zaidi, "Design and development of MATLAB Simulink based Selective Harmonic Elimination technique for three phase voltage source inverter," in *2013 International Conference on Advanced Computing and Communication Systems*, 2013, pp. 1-5: IEEE.

[6] I. J. Hasan, N. A. J. Salih, and N. I. Abdulkhaleq, "Three-phase photovoltaic grid inverter system design based on PIC24FJ256GB110 for distributed generation," *International Journal of Power Electronics Drive Systems (IJPEDS),* vol. 10, no. 3, pp. 1215-1222, 2019.

[7] Z. Li *et al.*, "A fast diagnosis method for both IGBT faults and current sensor faults in grid-tied three-phase inverters with two current sensors," *IEEE Transactions on Power Electronics,* vol. 35, no. 5, pp. 5267-5278, 2019.

[8] N. A. b. R. A. b. J. Z. b. R. T. Sutikno, "Reduction of total harmonic distortion of three-phase inverter using alternate switching strategy," *International Journal of Power Electronics and Drive System (IJPEDS),* vol. 12, no. 3, pp. 1598-1609, September 2021.

[9] I. Alhamrouni, M. B. Hamzah, M. Salem, A. Jusoh, A. B. Khairuddin, and T. Sutikno, "A bidirectional resonant converter based on wide input range and high efficiency for photovoltaic application," *International Journal of Power Electronics (IJPEDS),* vol. 10, no. 3, pp. 1469-1475, 2019.

[10] P. K. Roy, P. K. Saha, and A. Mondal, "Design of Closed-Loop Control of a Three-Phase Sine Wave Inverter Using High Gain DC–DC Converter for Renewable Energy Applications," in *Advances in Clean Energy Technologies*: Springer, 2021, pp. 281-292.

[11] N. Abd Rahim, K. Chaniago, and J. Selvaraj, "A modified H-bridge multilevel inverter for photovoltaic system," *IEICE Electronics Express,* vol. 7, no. 11, pp. 751-758, 2010.

[12] A. K. Yarlagadda and M. S. Chandana, "Design and Implementation of Arduino Based Three Phase Inverter " *International Journal of Electrical Electronics & Computer Science Engineering,* vol. 5, no. 1, p. 4, 2018.

[13] A. Dutta, "Some Aspects on 3-Phase Bridge Inverter (180 Degree Mode)," *International Journal of Engineering Inventions,* vol. 3, no. 4, pp. 1215-1222, 2013.

[14] N. Li, N. Zhi, H. Zhang, L. Su, W. Yue, and W. Zhao'an, "A novel conduction modes of three-phase six-switch Voltage Source Inverter," in *2015 IEEE 2nd International Future Energy Electronics Conference (IFEEC)*, 2015, pp. 1-4.

[15] G. P. Verma, S.P "Comparative Study of Different Firing Scheme for three Phase Voltage Source Inverter," *International Journal of Engineering Management Research,* vol. 5, no. 6, pp. 597-601, 2015.

[16] Krismadinata, Asnil, I. Husnaini, and E. Astrid, "Microcontroller Based 120^0 And 180^0 Conduction Modes Of Three-Phase Inverter For Photovoltaic Generation," *ARPN Journal of Engineering and Applied Sciences,* vol. 13, no. 11, p. 8, 2006.

[17] A. A. S. Helal, Mohamed H, "Dynamic voltage restorer adopting 150° conduction angle VSI," in *2008 IEEE Canada Electric Power Conference*, 2008, pp. 1-6: IEEE.

[18] E. M. a. V. Balaji, "Harmonic reduction in Three Phase Voltage Source Inverter by 150 degree conduction " *International Journal of Applied Theoretical Science and Technology* vol. 2, no. Issue 1, pp. 1001-1006, January 2016 2016.

[19] J. Trivedi, Ruchit Soni, M. Shah, and J. Shah, *Three Phase 150 Degree Mode of Conduction Voltage Source Inverter using Arduino*. 2016.

[20] D. G. Mangroliya, V. J. Rupapara, R. P. Akabari, and N. M. Vaghela, "An Advanced Three Phase Vsi With 1500 Conduction Mode Using PIC16F72," *Journal of Information, Knowledge And Research In Electrical Engineering,* vol. 2, no. 2, p. 6, 2012.

[21] M. H. Saied, M. Z. Mostafa, T. M. Abdel-Moneim, and H. A. Yousef, "On Three-Phase Six-Switches Voltage Source Inverter: A 150° Conduction Mode," in *2006 International Conference on Applied Electronics*, 2006, pp. 153-158.

[22] M. H. Rahman, M. A. Mannan, M. A. G. Khan, M. R. U. K. Shovon, and M. M. H. Mamun, "Design and Implementation of a Three-Phase Inverter Operated with Different Conduction Modes," in *2019 International Conference on Robotics,Electrical and Signal Processing Techniques (ICREST)*, 2019, pp. 346-349.

[23] R. Parikh, "Operation Overview of Three Phase Inverter With 120, 150 and 180 Conduction Mode," 2017.

[24] A. M. Patel, "THD Comparison for 180, 120 & 150 Degree Conduction Mode of Three Phase Inverter " *International Journal for Scientific Research & Development,* vol. 6, no. 3, p. 5, 2018.

[25] S. A. M. M. H, "Operation And Simulation Of Three Phase Inverter With 120°, 150° And 180° Conduction Mode," *International Journal Of Applied Research In Science And Engineering,* vol. 2, no. 7, pp. 733-739, 2017, Art. no. IJARSEV2I701.

[26] A. S. Makwana, "Comparative Harmonic Analysis of a 3-Phase Bridge Type Inverter Operating at different Conduction Mode using RL-Load," *International Research Journal of Engineering and Technology,* vol. 4, no. 5, pp. 2399-2407, 2017.

[27] E. M. Babaei, Mehdi "Improving Output Voltage of the Three Phase Six-Switch Inverters," *Telkomnika,* vol. 9, no. 3, 2011.

[28] S. D. A. Barve, "Design of Renewable energy source based inverter with 120^0 , 150^0 and 180^0 mode of conduction with and without filter " *International Journal of Science,*

ISSN: 1992-8645 www.jatit.org E-ISSN: 1817-3195

Engineering and Technology Research, vol. 2, no. 3, p. 10, 2013.

[29] M. H. Rahman, M. A. Mannan, and M. M. H. Mamun, "Design and Implementation of a Three-Phase Inverter Operated with different Conduction Modes with Automatic Powerfactor Improvement," *AIUB Journal of Science Engineering,* vol. 18, no. 2, pp. 44-48, 2019.

[30] P. Sen and P. Thakura, "Hardware design of three phase voltage source inverter using arduino microcontroller and its harmonic analysis," in *2018 Technologies for Smart-City Energy Security and Power (ICSESP)*, 2018, pp. 1-7: IEEE.